

Mathematical Analysis of Reactive and Non-Reactive Flow and Transport of Contaminants in Saturated Zone of Aquifers

Dr.Ramesh T

Department of Mathematics
Cambridge institute of technology
K R Puram, Bengaluru, India

Dr.Rekha J

Department of Mathematics
Cambridge institute of technology
K R Puram, Bengaluru, India

Dr. Shobhankumar D M

Department of Mathematics
Maharani Science College for women
Bengaluru, India

Dr. Rangaraju B V

Department of Mathematics
East Point College of Engineering
Bengaluru, India

ABSTRACT

In reactive and non-reactive aquifers with geo-hydrological favourable situations consisting of adequately permeable state between the soil surface & water table, it is every so often competitively priced to preciously recharge by means of the approach of basin permeation. A primary benefit of this approach is that a number of the dissolved and suspended solids are certainly eliminated for the duration of percolation by absorption and infiltration. The main equations of flow in porous media and transport within the saturated region in reactive and non-reactive aquifers are exposed to the non-linear moving boundary condition.

Even though the adaptability of arithmetical solutions, there are few problems associated with them, which include, numerical dispersion and diffusion at sharp fronts. In instances where geo-hydrological records are not appropriately sufficient known to defend the use of heterogeneous properties, the problems can be studied readily through suitable logical standards.

offered is decided by using relating them with existing experimental information and other models.

MATHEMATICAL EQUATIONS A.FLOW EQUATION

The continuity state in groundwater flow is given by

$$\frac{\partial q_i}{\partial x_i} = 0 \quad i = 1, 2, 3 \quad (1)$$

Where q_i is average velocity in i^{th} direction and x_i is Cartesian coordinate. In the work that trails, longitudinal coordinates in selected portions of the derivation are specified in the form, where x , y , z are used and taken as corresponding to x_1 , x_2 & x_3 , respectively, with x_3 - and z -directions vertically upwards.

By Darcy's law for anisotropic permeable medium, Equation (1) is of the form:

$$\frac{\partial}{\partial x_i} K \frac{\partial h}{\partial x_i} = 0 \quad (2)$$

Where K is the hydraulic conductivity and h is the piezo metric head.

The Pleasing benefit of symmetry, only half of the Figure (1) ($x \geq 0$) need to be involved in analysis and then, from Figure (1) and Equation (2) is exposed to the following circumstances:

Initial conditions:

$$h = a_0, \quad t = 0, \quad 0 \leq x \leq B, \quad 0 \leq z \leq a_0 \quad (3)$$

Symmetric

$$\frac{\partial h}{\partial x} = 0, \quad x = 0, \quad 0 \leq z \leq H \quad (4)$$

Water-resistant base:

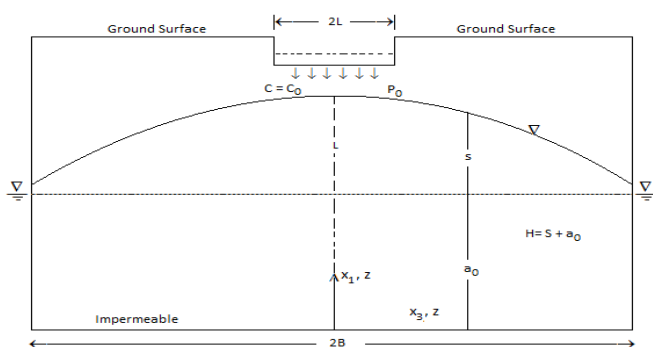


Figure 1 - Physical Configuration of Reactive Flow

INTRODUCTION

The aim of this chapter is to afford some analytical solutions for the reactive and non-reactive flow case as shown in figure 1. The figure denotes an extremely lengthy reactive aquifer, being recharged through an extremely lengthy recharge basin of width $2L$, with the aquifer confined by means of a drain of the regular head on both sides. Accurateness of the solutions

$$\frac{\partial h}{\partial z} = 0, \quad z = 0, \quad 0 \leq x \leq B \quad (5)$$

Uniform-head boundary:

$$h = a_0, \quad x = b, \quad 0 \leq z \leq a_0 \quad (6)$$

Discharge surface:

$$h = z, \quad x = B, \quad a_0 \leq z \leq H \quad (7)$$

Moving Free Space:

$$\left(R - \theta_e \frac{\partial H}{\partial t} \right) l_3 = K \frac{\partial h}{\partial x_i} l_i \quad (8)$$

With

$$R = \begin{cases} P_0, & 0 \leq x \leq L \\ 0, & x > L \end{cases} \quad (9)$$

$$\text{And } H = h = z \quad (10)$$

where a_0 is primary saturated depth, θ_e is actual permeability at free surface, R is permeation ratio function, P_0 is access rate from the basin, H is elevation of FS above reference datum, L is basin half-width, B is aquifer half-width, t is time, and l is unit external usual to the FS.

B. TRANSPORT EQUATION

The equation of solute transportation in permeable media (Bear, 1972) can written as:

$$\frac{\partial C}{\partial t} + u_i \frac{\partial C}{\partial x_i} = \frac{\partial}{\partial x_i} D'_{ij} \frac{\partial C}{\partial x_j} \quad (11)$$

Where C is solute absorption, D'_{ij} is hydro dynamic dispersion coefficients, and u_i is the minute opening average velocity.

Factors u_i and D'_{ij} are defined as:

$$u_i = \frac{-K}{\theta_r} \frac{\partial h}{\partial x_i} \quad (12)$$

$$D'_{ij} = a_{ijkl} \frac{u_k u_l}{|u|} + T D_d \delta_{ij} \quad (13)$$

Where θ_r is the Darcy permeability, a_{ijkl} the dispersivity tensor, $|u|$ is degree of minute opening velocity, T is tortuosity, D_d is coefficient of nuclear diffusion, and δ_{ij} is Kronecker delta. The word "Darcy porosity" denotes the real hydraulically connected minute opening space in the saturated region. It is stated by Jacob Bear and others as the "effective porosity"; though, to discriminate it from the "effective porosity" at the FS the term "Darcy porosity" is accepted in this thesis.

In Figure 1, Equation (11) is subjected to the subsequent ICs:

$$C = 0, \quad t = 0, \quad 0 \leq x \leq B, \quad 0 \leq z \leq a_0 \quad (14)$$

Symmetric

$$\frac{\partial C}{\partial x} = 0, \quad x = 0, \quad 0 \leq z \leq H \quad (15)$$

Impermeable base boundary:

$$\frac{\partial C}{\partial z} = 0, \quad z = 0, \quad 0 \leq x \leq B \quad (16)$$

Seepage surface:

$$\frac{\partial C}{\partial x} = 0, \quad x = B, \quad a_0 \leq z \leq H \quad (17)$$

Exit end boundary:

$$\left(u_i C - D_d \frac{\partial C}{\partial x_i} \right) l_i \Big|_{outside} = \theta_r \left(u_i C - D'_{ij} \frac{\partial C}{\partial x_i} \right) l_i \Big|_{inside}, \quad x = b, \quad 0 \leq z \leq a_0 \quad (18)$$

Free surface boundary:

$$-D'_{ij} \frac{\partial C}{\partial x_j} l_i = \left(P_0 + \theta_{initial} \frac{\partial H}{\partial t} \right) \frac{l_3}{\theta_r} (C - C_0), \quad 0 \leq x \leq L, \quad \frac{\partial H}{\partial t} \geq 0$$

$$-D'_{ij} \frac{\partial C}{\partial x_j} l_i = \frac{\theta_{initial}}{\theta_r} \frac{\partial H}{\partial t} l_3 (C - C_{unsat}), \quad L < x \leq B, \quad \frac{\partial H}{\partial t} \geq 0$$

$$-D'_{ij} \frac{\partial C}{\partial x_j} l_i = 0, \quad L < x \leq B, \quad \frac{\partial H}{\partial t} < 0 \quad (19)$$

Where Initial -- pore space filled by moistness,

C_0 -- the initial solute concentration

C_{unsat} -- the solute concentration in the unsaturated region above the Free Space

$$\theta_{Total} \cong \theta_r = \theta_e + \theta_{initial}$$

In which θ_{Total} is the total porosity associated.

C. MATHEMATICAL SOLUTIONS

A. FLOW EQUATION

The improvement of solutions for transportation equation ought to be pre yielded by the solution of the flow equation for the reason that later governs the velocity dispersal.

The growth of the Free Space above the preliminary saturated intensity, s , is first received with the aid of making use of the Dupuit-Forcheimer assumption. The resultant equation has then linearized the use of the idea that $s/a_0 \ll 1$ that is usually real for small infiltration rates. The usage of Equations from (2) to (10), of the form:

$$\frac{K a_0}{\theta_e} \frac{\partial^2 s}{\partial x^2} = \frac{\partial s}{\partial t} - \frac{R}{\theta_e} \quad (20)$$

Subjected to the circumstances:

$$\begin{aligned} s &= 0, & t &= 0, \quad 0 \leq x \leq B \\ \partial s / \partial x &= 0, & x &= 0 \\ s &= 0, & x &= B \\ R &= P_0, & 0 \leq x \leq L \\ R &= 0, & L \leq x \leq B \end{aligned}$$

A solution to Equation (20) and its boundary circumstances is required over the Eigen function expansion technique to give:

$$s = \sum_{n=1}^{\infty} \frac{4P_0}{\theta_e(2n-1)\pi} \sin\left(\frac{2n-1}{2B}\pi L\right) \cos\left(\frac{2n-1}{2B}\pi x\right) \left(1 - \exp(-\alpha t)\right) \quad (21)$$

$$\text{Where } \alpha = \frac{Ka_0}{\theta_e} \left(\frac{2n-1}{2B}\pi\right)^2$$

The site of the higher boundary of the entire saturated flow area is now described by Equation (21). But, the Dupuit-Forchheimer hypothesis implies a horizontal flow velocity through the flow area. This isn't really a especially below the basin in which the vertical components predominates.

A more precise explanation of the velocity distributions must be required

It is now supposed that the flow design at any time t can be defined hence:

$$u_i(x, z, t) = u_i(x, z, \infty) f(t) \quad (22)$$

Where $f(t)$ is the scale function reliant on time.

Velocity at stable state $u_i(x, z, \infty)$ is pursued thru a easy flow area, with the resulting transformation:

$$X \equiv x, \quad Z = za_0/(s+a_0) \quad (23)$$

This conversion maps the flow area onto a rectangular area as indicated in the following Figure (2).

Using Equation (23), Equation (2) and the suitably transformed boundary conditions Equations (3) to (10) are still not agreeable to analytical solution methods and further interpretation of the problem is needed.

Based on the principle that is $s/a_0 \ll 1$, the added expectations are discussed below.

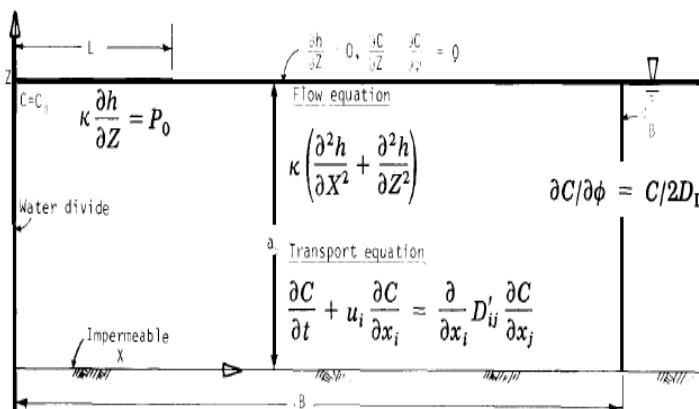


Figure 2 –Physical transformation of the domain

The unsteady free surface may be roughly defined through a circulation line which infers that the flow design is corresponding to the reactive case.

Based on these norms, only the stable-state velocity design in the estimated restricted area figure (2) be required, and the downstream end can be prolonged to infinity.

Equation (2) and its related boundary situation are simplified to:

$$\kappa \left(\frac{\partial^2 h}{\partial X^2} + \frac{\partial^2 h}{\partial Z^2} \right) = 0, \quad 0 \leq X \leq \infty, \quad 0 \leq Z \leq a_0 \quad (24)$$

$$\kappa \frac{\partial h}{\partial Z} = P_0, \quad 0 \leq X \leq L, \quad Z = a_0 \quad (25)$$

And the remaining part of the boundary is resistant. Equation (24) and the boundary conditions can be resolved using the Schwarz-Christoffel transformation method. Particulars of the solution process have been given

Variant part of the 1st term of equation (21), i.e.

$$f(t) = 1 - \exp(-\alpha_1 t) \quad \text{Somewhere else} \quad (\text{Guvanasen, 1983}).$$

Solutions in terms of relations between X, Z, ϕ , and ψ are:

$$X = \frac{a_0}{\pi} \ln(\sqrt{\xi} + \sqrt{1+\xi}) \quad (26)$$

$$z = \frac{a_0}{\pi} \cos^{-1}[\gamma_1 / \cosh(\pi X / a_0)] \quad (27)$$

$$\phi = \frac{Q}{\pi} \ln(\sqrt{\mu} + \sqrt{1+\mu}) \quad (28)$$

And

$$\psi = \frac{Q}{\pi} \cos^{-1}[\lambda_1 / \cosh(\pi \phi / Q)] \quad (29)$$

where

$$\gamma_1 = \varepsilon_1 \cosh(\pi \phi / Q) \cos(\pi \psi / Q) + \varepsilon_2; \quad \gamma_1 = \varepsilon_1 \sinh(\pi \phi / Q) \sin(\pi \psi / Q)$$

$$\xi = \frac{1}{2} \left\{ (\gamma_2^2 + \gamma_1^2 - 1) + [(\gamma_2^2 + \gamma_1^2 - 1)^2 + 4\gamma_2^2]^{\frac{1}{2}} \right\}$$

$$\varepsilon_1 = -\frac{1}{2} [1 - \cosh(\pi L / a_0)]; \quad \varepsilon_2 = -\frac{1}{2} [1 + \cosh(\pi L / a_0)]$$

$$\lambda_1 = \frac{1}{\varepsilon_1} \cosh(\pi X / a_0) \cos(\pi Z / a_0) - \varepsilon_2 / \varepsilon_1;$$

$$\lambda_2 = \frac{1}{\varepsilon_1} \sinh(\pi X / a_0) \sin(\pi Z / a_0)$$

$$\mu = \frac{1}{2} \left\{ (\lambda_2^2 + \lambda_1^2 - 1) + \left[(\lambda_2^2 + \lambda_1^2 - 1)^2 + 4\lambda_2^2 \right]^{1/2} \right\}$$

$$Q = P_0 L / \theta_r$$

The velocity along streamlines is given by:

$$u(\phi, \psi; t \rightarrow \infty) = \frac{Q}{\varepsilon_1 a_0} \frac{\left[(\lambda_2^2 + \lambda_1^2 - 1)^2 + 4\lambda_2^2 \right]^{1/4}}{\left[\cosh^2(\pi \phi / Q) \sin^2(\pi \psi / Q) + \sinh^2(\pi \phi / Q) \cos^2(\pi \psi / Q) \right]^{1/2}} \quad (30)$$

Then

$$u_\phi = \sqrt{u_x^2 + u_z^2}$$

and the assumptions in equation (22) state that:

$$u_\phi(t) = u_\infty f(t) \quad (31)$$

where $u_\infty = u_\phi(\phi, \psi; t \rightarrow \infty)$.

In this study, u_∞ is given in the equation (30) and

$f(t)$ is approached by the time (32)

Where $\alpha_1 = K a_0 \pi^2 / (\theta_e 4 B^2)$.

Henceforth the flow area is now well-defined by given geometrical limitations and Equation (21), the flow design is defined by Equation (26) – (29), and the velocity distribution is defined by Equations (31) and (32).

B. Transport Equation

Applying the transformation in Equation (23) to (11), we get

$$C(x, z, t) = C^*(X, Z, t)$$

Where C and C* are absorptions in the original and altered areas respectively. Related with such a many relations, they are:

$$\frac{\partial C}{\partial t} = \frac{\partial C^*}{\partial t} + \frac{\partial C^*}{\partial Z} \frac{\partial Z}{\partial t};$$

$$\frac{\partial C}{\partial x} = \frac{\partial C^*}{\partial X} + \frac{\partial C^*}{\partial Z} \frac{\partial Z}{\partial X};$$

$$\frac{\partial C}{\partial z} = \frac{\partial C^*}{\partial Z} \frac{a_0}{H}; \quad \frac{\partial Z}{\partial t} = -\frac{Z}{H} \frac{\partial H}{\partial t};$$

And

$$\frac{\partial Z}{\partial X} = -\frac{Z}{H} \frac{\partial H}{\partial x};$$

To resolve the transportation equation, it is required that:

$$\partial(\cdot) / \partial d = \partial(\cdot)^* / \partial D$$

Where D = X, Z, t and d = x, z, t

To attain the above state certain expectations have to be made:

$$a_0 / H \approx 1 \quad \text{i.e., } s / a_0 \ll 1$$

$\partial H / \partial x \approx 0$ i.e., the gradient of surface is very small.

$$\partial H / \partial t \approx 0$$

I.e. the rate of growth of the FS is very small, which is realistic when the flow rate is small and $s / a_0 \ll 1$.

Having completed the above norms, the transformed area of the transport equation

(Figure 2) stated, by removing asterisks, as:

$$\frac{\partial C}{\partial t} + u_i \frac{\partial C}{\partial X_i} = \frac{\partial}{\partial X_i} D'_{ij} \frac{\partial C}{\partial X_j} \quad (33)$$

For Reynolds numbers, above 10^{-3} of molecular diffusion is insignificant related with convective dispersion. Equation (13) by using equation (22), can be rewritten as:

$$D'_{ij} = \left(a_{ijkl} \frac{u_k u_l}{|u|} \right)_{t=\infty} \cdot f(t) \quad (34)$$

By the transformation:

$$\tau = \int_0^t f(t) dt$$

And Equations (22) and (34), Equation (33) is of the form:

$$\frac{\partial C}{\partial \tau} + u_i(X, Z, \infty) \frac{\partial C}{\partial X_i} = \frac{\partial}{\partial X_i} D'_{ij}(X, Z, \infty) \frac{\partial C}{\partial X_j} \quad (35)$$

It can be stated in a curvilinear coordinate system as:

$$\frac{\partial C}{\partial t} + u_\infty^2 \frac{\partial C}{\partial \phi} = u_\infty^2 \left[\frac{\partial}{\partial \phi} \left(D_L \frac{\partial C}{\partial \phi} \right) + \frac{\partial}{\partial \psi} \left(D_T \frac{\partial C}{\partial \psi} \right) \right]$$

(36)

Where DT and DL are the lateral and longitudinal direction hydrodynamic dispersal coefficients.

Supposing that there is no dispersion throughout streamlines, Equation (36) becomes

$$\frac{\partial C}{\partial \tau} + u_\infty^2 \frac{\partial C}{\partial \phi} = u_\infty^2 \frac{\partial}{\partial \phi} \left(D_L \frac{\partial C}{\partial \phi} \right) \quad (37)$$

The boundary conditions, Equations from

(12) to (19), to which Equation (37) is subjected to:

$$u_{\infty(\phi \rightarrow \infty)} = v_{\infty} = P_0 L / (\theta_T a_0) \quad (38)$$

Since DL is constant we can take outside from differentiation in Equation (37).

The boundary condition upstream, equation (19), is equivalent to:

$$C(\phi = 0, \tau) = C_0 \quad (39)$$

Which is corresponding to θ_{initial} and a concentration gradient across the boundary approaching to zero.

At the perpendicular downstream end (Equation 18) with $\phi = \phi_B$:

$$\frac{\partial C}{\partial \phi} = \frac{C}{2D_L} \quad (40)$$

The real boundary condition needs to be inferring concentration at once inside the domain equals that right away outside. But, to enable the mathematical answer the approximation in Equation (40) is hired. This estimate is authentic for decrease values of C.

Lapidus (1966) confirmed that a solution using the zero-gradient boundary situation is too viable. Their answer, though, essential roots from the related non-linear equation. Due to the relative comfort with which the solution using Equation (40) may be computed, and the verified accuracy of the ensuing answer in comparison with experimental results, Equation (40) is used because of the boundary circumstance.

Initial Conditions:

$$C(\phi, \tau = 0) = 0 \quad (41)$$

Other boundary conditions in Equations from (3) to (17) and (19) are accepted by virtue of the foregoing approximations.

Put $\beta = v_{\infty}^2 \tau$ Equation (37) is transformed to:

$$\frac{\partial C}{\partial \beta} + \frac{\partial C}{\partial \phi} = D_L \frac{\partial^2 C}{\partial \phi^2} \quad (42)$$

Let us consider the result in the form:

$$C(\phi, \beta) = \chi(\phi, \beta) \exp(\phi / 2D_L - \beta / 4D_L) \quad (43)$$

Equation (42) and initial and boundary conditions become:

$$\frac{\partial \chi}{\partial \phi} = D_L \frac{\partial^2 \chi}{\partial \phi^2}; \quad \chi(\phi, 0) = 0 \quad (44)$$

$$\chi(0, \beta) = C_0 \exp\left(\frac{\beta}{4D_L}\right); \quad \frac{\partial \chi}{\partial \phi}(\phi_B, \beta) = 0 \quad (45)$$

By Laplace transformation with respect to β , using equation (44) becomes

$$\bar{\chi}(0, r) = D_L \frac{d^2 \bar{\chi}}{d\phi^2} \quad (46) \text{ Equation}$$

(45) become

$$\bar{\chi}(0, r) = 1 / \left(r - \frac{1}{4D_L} \right) \quad (47)$$

$$d\bar{\chi}/d\phi = 0; \quad \phi = \phi_B \quad (48)$$

Where

$$\bar{\chi} = \int_0^{\infty} \exp(-r\beta) \chi \, d\beta$$

With r = parameter of transformation. Solving Equations from (46) to (48) gives:

$$\bar{\chi} = \frac{C_0}{(r - 1/4D_L)} \frac{\cosh(\phi_B - \phi) \sqrt{r/D_L}}{\cosh[\phi_B \sqrt{r/D_L}]} \quad (49)$$

By inverse Laplace transformation, we get

$$\chi = C_0 \exp\left(\frac{\beta}{4D_L}\right) \sum_{n=-\infty}^{\infty} \frac{(-1)^n}{2} \left[\exp\left(\frac{\phi_B - \phi + (2n-1)\phi_B}{2D_L}\right) \right] \operatorname{erfc}\left(\frac{-(\phi_B - \phi + (2n-1)\phi_B) - \beta}{2\sqrt{D_L\beta}}\right) + \exp\left(\frac{-(\phi_B - \phi + (2n-1)\phi_B)}{2D_L}\right) \operatorname{erfc}\left(\frac{-(\phi_B - \phi) + (2n-1)\phi_B + \beta}{2\sqrt{D_L\beta}}\right) \quad (50)$$

From Equation (43), and noting that $\beta = v_{\infty}^2 \tau$,

Equation (50) becomes

$$C(\phi, \tau) = C_0 \exp\left(\frac{\phi}{2D_L}\right) \sum_{n=-\infty}^{\infty} \frac{(-1)^n}{2} \left\{ \exp\left(\frac{(-\phi + 2n\phi_B)}{2D_L}\right) \operatorname{erfc}\left(\frac{(\phi - 2n\phi_B - v_{\infty}^2 \tau)}{2v_{\infty} \sqrt{D_L \tau}}\right) + \exp\left(\frac{(\phi - 2n\phi_B)}{2D_L}\right) \operatorname{erfc}\left(\frac{(\phi - 2n\phi_B + v_{\infty}^2 \tau)}{2v_{\infty} \sqrt{D_L \tau}}\right) \right\} \quad (51)$$

A good approximation is

$$C = \frac{C_0}{2} \left\{ \operatorname{erfc} \left(\frac{(\phi - v_\infty^2 \tau)}{2v_\infty \sqrt{D_L \tau}} \right) + \exp \left(\frac{\phi}{D_L} \right) \operatorname{erfc} \left(\frac{(\phi + v_\infty^2 \tau)}{2v_\infty \sqrt{D_L \tau}} \right) \right\} \quad (52)$$

The longitudinal dispersion factor, D_L , in S1 and S2 is approximated by:

$$D_L = a_1 d_{50} u_\infty$$

Which resembles to $B \rightarrow \infty$.

(b) Solution 2 (S2). Interpretations used in developing this solution are

The downstream end can be prolonged to $\phi = \infty$;

The convective procedure is main so that:

$$\frac{\partial}{\partial \phi} = -\frac{1}{u_\infty^2} \frac{\partial}{\partial \tau} \quad (53)$$

This technique adopts that as the tracer actions far away from the basis, the impacts of dispersion on the tracer distribution because the tracer actions beyond any factor end up small in contrast to the entire dispersion as much as that point.

With the help of equation (53), equation (42) becomes:

$$\frac{\partial C}{\partial \tau} + u_\infty^2 \frac{\partial C}{\partial \phi} = \frac{D_L}{u_\infty^2} \frac{\partial^2 C}{\partial \tau^2} \quad (54)$$

Which is subjected to

$$\begin{aligned} C &= C_0, & \phi &= 0 \\ C(\phi, 0) &= 0 \\ \partial C / \partial \tau &= 0, & \tau &= 0 \end{aligned} \quad (55)$$

By Laplace transformation with respect to r , using equation (55) and equation (54) becomes

$$r \bar{C}(\phi, r) + u_\infty^2 \frac{d\bar{C}}{d\phi}(\phi, r) = \frac{D_L}{u_\infty^2} r^2 \bar{C}(\phi, r) \quad (56)$$

Equation (55) becomes:

$$\bar{C}(0, r) = \frac{C_0}{r} \quad (57)$$

Where

$$\bar{C}(\phi, r) = \int_0^\infty \exp(-r\tau) C(\phi, \tau) d\tau$$

Solving equation (56) and (57), we obtain:

$$\bar{C}(\phi, r) = \frac{C_0}{r} \exp(-\eta_1 r + \eta_2 r^2) \quad (58)$$

Where

$$\eta_1 = \int_0^\phi \frac{d\phi}{u_\infty^2} \quad \text{And} \quad \eta_2 = \int_0^\phi \frac{D_L}{u_\infty^4} d\phi$$

By inverse Laplace transformation of equation (58) we obtain

$$C = \frac{C_0}{2} \left[\operatorname{erf} \left(\eta_1 / \sqrt{4\eta_2} \right) + \operatorname{erf} \left((\tau - \eta_1) / \sqrt{4\eta_2} \right) \right] \quad (59)$$

Where a_1 is longitudinal dispersity constant, and d_{50} the 50percent finer diameter of the aquifer substantial. The above equations is built on the experimental data and linearized to obey with equation (13).

RESULTS AND DISCUSSIONS

Concentrations contours generated by way of solutions S1 and S2, described in Equations (3.51) and (3.59), correspondingly, are indicated in Figure 3.3. In which the situations of the FS are produced through equation (3.21). Underneath the basin, at initial stages of recharge, the contours from the two solutions are comparable. Because the front movements further far away from the basin, at more times, locations of the front defined with the aid of each solution are inside the equal area however, of various upright distribution. The front defined by means of S1 is near vertical with its function about consistent with the average function of the front defined by S2.

Results from S1 and S2 are actually in comparison with statistics from trials in a sand box in which a matrix of conductivity investigations is fixed. Details of the experiments are given.

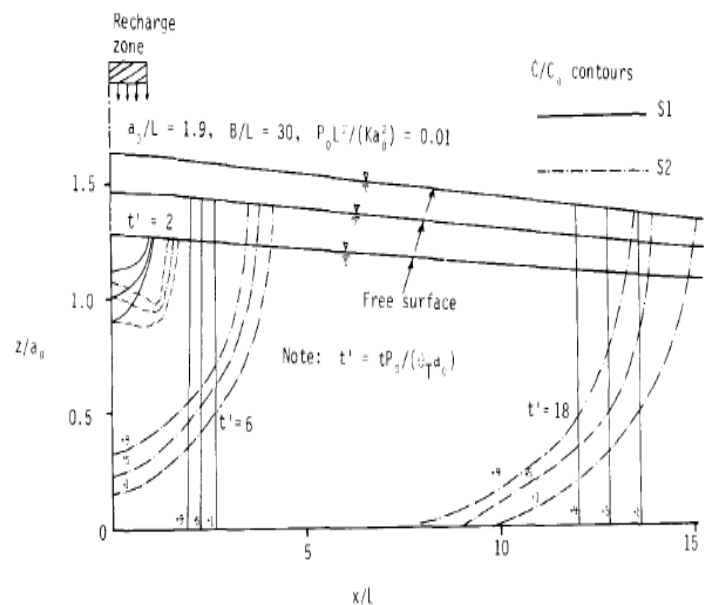


Figure 3 – Concentration contours generated by analytical solutions, S1 and S2 at various times

Presented here are outcomes from 2 experiments A and B, the particulars of which are given in table 1. A regular evaluation amongst the measured and the calculated breakthrough curves is indicated in Fig.4 in which it's far obvious that the grades of the leap forward curves are correctly pretended through the theoretical solutions. Because of the similarity of the breakthrough curve slopes, the exactness of the theoretical answers may be measured using a feature arrival time at each probe place. Theoretic and experimental arrival times of $C/C_0 = 0.5$ from experiments A and B are displayed in 5A and 5B,

respectively. SJ usually does better under the basin ($x/L < 1$) however as the front travels similarly far away from the basin both solutions agree equally well with the experimental effects, despite the fact that SJ can't signify the vertical distribution of solute concentration.

Table 1: Details of Experiments

Experiment	a_0 (mm)	L (mm)	B (mm)	θ_e
A	308	300	6,000	0.3029
B	164.5	300	6,000	0.325
$a_I=1.75, d_{50}=1.88\text{mm}$				

It is noted also that as the value of $p' = P_0 L^2 / (K a_0^2)$ increases the discrepancies among the intended and the experimental arrival times are more suggested. This was observed from many similar experiments with distinct values of p' .

It has been proven that the float and transfer of solute in free-range aquifers can fairly correctly pretend with the aid of the finite-element method Equations. (2) – (19) are solved without simplifying assumptions.

The evaluation among concentration contours expected by means of S1 and S2 and the finite - element solution using the information from expt. As indicated in fig 6A. And 6B which makes use of data from experiment B highlights the mentioned difference among the finite-element result and the analytical results S1 and S2 while p' is huge. At the selected time as indicated in fig 6B, the S1 and S2 fronts lag drastically behind the finite-element front.

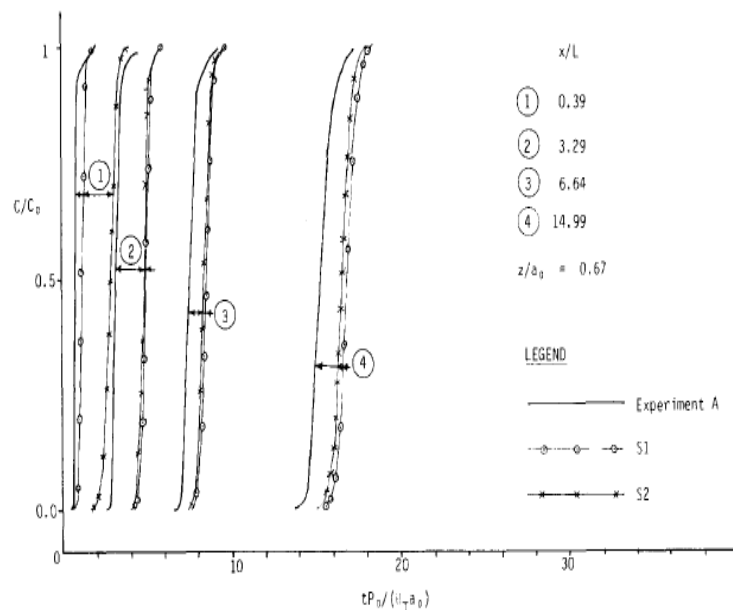


Figure 4 – Comparison between theoretical and experimental Break-through-curves

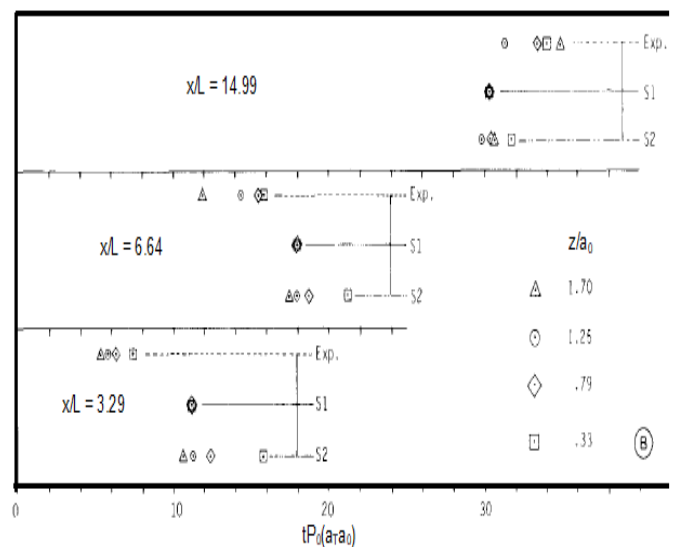
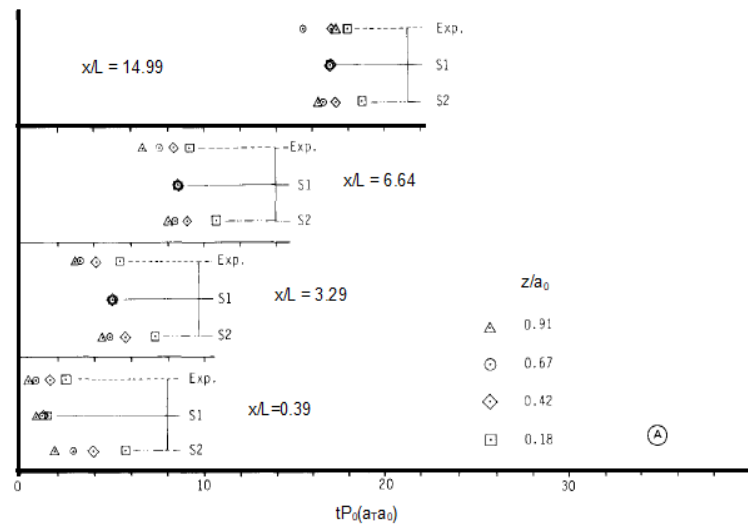


Figure 5: Comparison of theoretical and experimental arrival times of $C/C_0 = 0.5$
(A) Experiment - A (B) Experiment - B

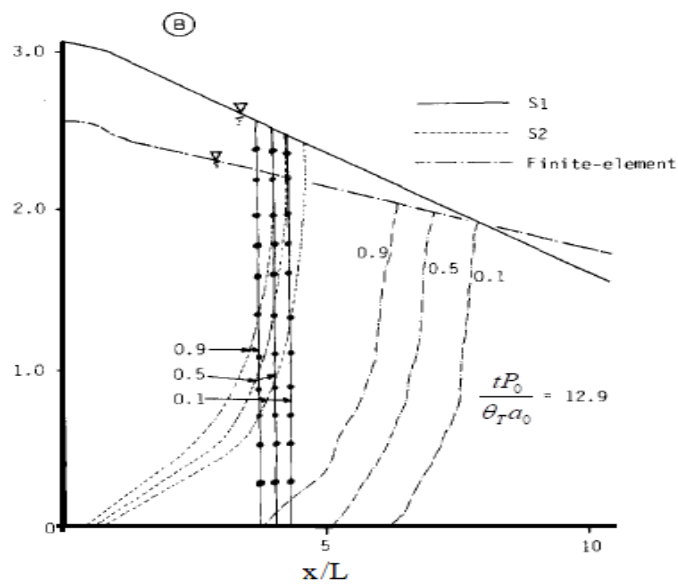


Figure 6: Comparison between analytical and finite-element solutions:

(A) Experiment – A and (B) Experiment - B

REFERENCES

- [1] B. Hunt, Contaminant source solutions with scale-dependent dispersivities, J. Hydrologic Engg., 3 (4) (1998) 268-275.
- [2] J. L. Hutson, and A. Cass, A retentively functions for use in soil-water simulation models, J. Soil Sci., 38 (1987) 105 - 113. [3] R. A. Freeze, and J. A. Cherry, Groundwater, Prantice Hall, Inc., New Jersey, USA (1979).
- [4] G. E. Grisak, and J. F. Pickens, Cherry, Solute transport through fractured media, @ common study of fractured till. Water Resour. 16(4) (1980) 731-739.
- [5] G. W. Sposito, A. Jury, and V.K. Gupta, Fundamental Problems in the stochastic convection-dispersion model of the solute transport in aquifers & field soils, Water Resource Res., 22 (1986) 77- 88. 176 T.Ramesh et al. / IJMTT, 67
- (7), 169-177, 2021 [6] S. R. Sudheendra, A solution of the differential equation of longitudinal dispersion with variable coefficients in a finite domain, Int. J. of Applied Mathematics & Physics, 2(2) (2010) 193-204.
- [7] S. R. Sudheendra, A solution of the differential equation of dependent dispersion along uniform and non-uniform flow with variable coefficients in a finite domain, Int. J. of Mathematical Analysis, 3(2) (2011) 89-105.
- [8] S. R. Sudheendra, An analytical solution of one-dimensional advection diffusion equation in a porous media in presence of radioactive decay, Global Journal of Pure and Applied Mathematics, 8(2) (2012) 113-124.
- [9] S. R. Sudheendra, J. Raji, C.M. Niranjana, Mathematical Solutions of transport of pollutants through unsaturated porous media with adsorption in a finite domain, Int. J. of Combined Research & Development, 2(2) (2014) 32-40.
- [10] S. R. Sudheendra, M. Praveen Kumar, and T. Ramesh, Mathematical Analysis of transport of pollutants through unsaturated porous media with adsorption and radioactive decay, Int. J. of 01- 08. Combined Research & Development, 2(4) (2014)